SPi	Journal Code				Article ID				
	W	E			2	2	9	6	No. of Pages: 13	ME:

Received: 3 July 2018 | Revised: 28 August 2018 | Accepted: 29 October 2018

DOI: 10.1002/we.2296

RESEARCH ARTICLE

WILEY

Initialization of DFIG wind turbines with a phasor-based approach analysis and comparison with the traditional Newton–Raphson algorithm

Alejandro Rolán[1] | Joaquín Pedra[2]

[1] Department of Industrial Engineering, Institut Quimic de Sarria, Ramon Llull University, Barcelona, Spain

[2] Department of Electrical Engineering, Universitat Politècnica de Catalunya, Barcelona, Spain

Correspondence
Alejandro Rolán, Department of Industrial Engineering, Institut Quimic de Sarria, Ramon Llull University, Via Augusta 390, Barcelona 08017, Spain.
Email: alejandro.rolan@iqs.url.edu

Abstract

The objective of this paper is to propose a simple approach to solve the steady state of a wind turbine (WT) equipped with a doubly fed induction generator (DFIG), which can be used to initialize dynamic studies of the machine. The idea is to model the rotor-side converter (RSC) as a constant current source connected to the rotor of the DFIG. The resulting equivalent circuit consists of a voltage source in series with a reactance, which makes it possible to obtain simple phasor expressions that can be used to obtain the Park components of the variables. The proposed method is compared with the traditional Newton–Raphson algorithm, showing that it is easier and faster to implement, as it makes use of the phasor expressions and it does not require an iterative process to obtain the final solution. Finally, the results of the proposed method are used to simulate a 2-MW DFIG-based WT under three-phase faults, considering three different WT-operating points. In these simulations, the idea of constant rotor current is extrapolated to the entire event. The simulated results show that both current at torque peaks are reduced. The analytical study and the simulations have been carried out in MATLAB™.

KEYWORDS

doubly fed induction generator (DFIG), initialization, steady-state conditions, wind energy

1 | INTRODUCTION

Wind turbines (WTs) equipped with doubly fed induction generators (DFIGs) is the most common technology utilized nowadays in wind energy conversion systems.[1] Because of the increase of renewable energy units into the distribution grids during the last years, the grid operators have created grid codes in order to make these systems meet fault ride-through capability; that is, WTs must keep connected to the main grid when disturbances occur.[2] For this reason, the understanding of WTs equipped with DFIGs under faults in the main grid is the first step to ensure a continuous injection of electricity in order to improve power quality for electricity consumers.[3]

The most complete model when describing induction machines is the fifth-order (or full-order) model, which implies that five equations are needed: four electrical equations (two related to stator and two related to the rotor) plus the mechanical equation. The classical approach to reduce the complexity of this model is to neglect the derivatives of the stator fluxes, which results in the well-known third-order model.[4] Regarding DFIGs, a comparison between the fifth-order model and the third-order model is detailed in Ekanayake, Holdsworth, and Jenkins.[5]

The present study considers the full-order model of the machine. Besides, the rotor-side converter (RSC) is modeled as a constant current, with the aim of providing a simple control to reduce the current and torque peaks that usually appear on grid-connected equipment under fault conditions.[6,7] However, the control of the DFIG is out of the scope of this paper, as it is focused on solving the steady-state conditions. For a more detailed explanation about vectorial control of DFIGs for WT applications, the work done by Pena, Clare, and Asher[8] can be consulted.

When neglecting the derivative terms of the fifth-order (or full-order) model of the DFIG, the steady-state model is obtained. This model, written in *dq* components (using the Park transformation in the synchronous reference frame), is based on a set of nonlinear equations, which implies that an iterative process is needed to find the analytical solution. This is achieved by the Newton–Raphson algorithm.[9] Steady-state models in the literature usually follow this method.[10-12] A different method is presented in Feijóo, Cidrás, and Carillo[13] where it does not make use of the *dq* components, but it still needs an iterative process to obtain the analytical solution. In the study of Slootweg, Polinder, and Kling,[14] it is shown a procedure to initialize WTs with different electrical generators for power system dynamic simulations, but it makes reference to an iterative process to obtain the final solution. In the study of Amutha and Kalyan,[15] a method for obtaining steady-state solution with four unknown variables is presented, but this method is based on power flow analysis, so the DFIG is modeled using a reduced-order model (from the point of view of an electrical power system). A recent method proposed by Wu and Xie[16] suggests calculating steady-state operating conditions for eigenvalue analysis of DFIG-based WTs without making use of an iterative process, just by ignoring the dynamic terms of the equations. In the study of Han, Cheng, Wei, and Jian,[17] the steady state model of a specific DFIG, named dual-stator brushless DFIG is proposed, which appears to be a good machine to get rid of harmonics for wind applications.

The present paper focuses on the use of the per-phase steady-state equivalent circuit of a DFIG with a constant current (which models the RSC) connected to the rotor of the machine. The resulting circuit consists of a voltage source in series with a reactance, by means of which it is possible to obtain quite simple phasor expressions for the stator current, rotor current, and rotor voltage. Finally, from these expressions it is possible to obtain the *dq* components (in the synchronous reference frame) of the variables to initialize dynamic studies.

The proposed method is compared with the traditional Newton–Raphson algorithm. It is shown that the presented approach is easier and faster to implement, as it makes use of the phasor expressions and it does not require an iterative process to obtain the final solution, giving similar results.

Finally, once the steady-state values are obtained in *dq* components, they are used to initialize the dynamic study of a 2-MW DFIG-based WT. This WT is simulated connected to a transmission grid where a three-phase fault originates. As the sag has a short duration (just a few cycles), the mechanical speed of the machine is assumed to be constant. Moreover, the idea of constant rotor current is applied during the entire event, with the aim of reducing both current and torque peaks.

2 | DFIG DYNAMIC MODEL

Figure 1 shows the general scheme of a variable-speed WT equipped with a DFIG. It consists of rotor blades, gearbox, generator, and power converter. The converter module has a RSC, a direct current (DC) link, and a grid-side converter (GSC). The DFIG is connected to the grid at point of common connection (PCC) through its stator and its GSC. **F1**

The DFIG dynamic equations written in *dq* components using the Park transformation in the synchronous reference frame (see appendix for more details) and considering the motor sign convention are as follows:

$$\begin{aligned}
v_{sd} &= (R_s + L_s p) i_{sd} + M p i_{rd} - L_s \omega_s i_{sq} - M \omega_s i_{rq},\\
v_{sq} &= (R_s + L_s p) i_{sq} + M p i_{rq} + L_s \omega_s i_{sd} + M \omega_s i_{rd},\\
v_{rd} &= (R_r + L_r p) i_{rd} + M p i_{sd} - L_r s \omega_s i_{rq} - M s \omega_s i_{sq},\\
v_{rq} &= (R_r + L_r p) i_{rq} + M p i_{sq} + L_r s \omega_s i_{rd} + M s \omega_s i_{sd},\\
\Gamma_m &= \wp M (i_{rd} i_{sq} - i_{rq} i_{sd}),
\end{aligned} \tag{1}$$

where $p = d/dt$ is the derivative operator, $\omega_s = 2\pi f_s$ is the grid pulsation ($T = 1/f_s$ is the grid period), $\wp$ is the DFIG pole pairs, Γ_m is the electro-magnetic torque, the subscript s and r stand for the stator and for the rotor, respectively; the subscripts d and q stand for the direct and quadrature components of the Park variables, respectively, and $s = (\omega_s - \wp\, \omega_m)/\omega_s$is the DFIG slip. The DFIG dynamic equations in Equations 1 can be represented by the equivalent circuits depicted in Figure 2, where $\phi_{sd} = L_s\, i_{sd}$, $\phi_{sq} = L_s\, i_{sq}$, $\phi_{rd} = L_r\, i_{rd}$, and $\phi_{rq} = L_r\, i_{rq}$. **F2**

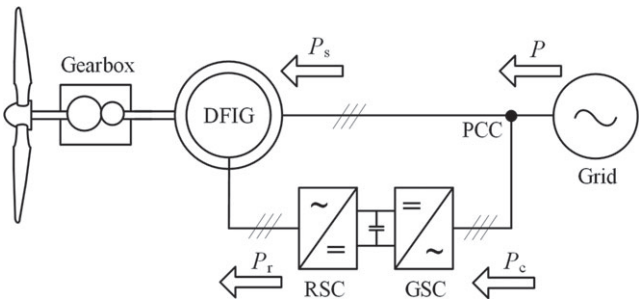

FIGURE 1 Doubly fed induction generator (DFIG)-based wind turbine with the representation of active powers, considering motor sign convention

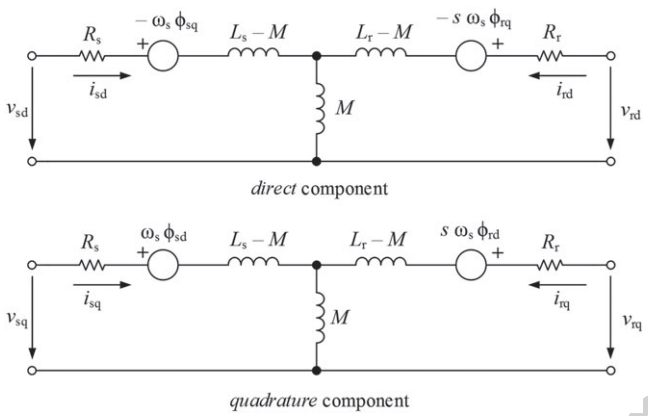

FIGURE 2 Equivalent circuit of the doubly fed induction generator (dynamic model) in Park variables (*dq* components), considering synchronous reference frame and motor sign convention

The instantaneous active power, p, and reactive power, q, exchanged between the WT and the grid is given by:

$$\begin{aligned} p &= p_s + p_c = v_{sd} i_{sd} + v_{sq} i_{sq} + v_{rd} i_{rd} + v_{rq} i_{rq} \\ q &= q_s + q_r = v_{sq} i_{sd} - v_{sd} i_{sq}, \end{aligned} \tag{2}$$

where the power losses in the converter are neglected, ie, $p_c = p_r$ and the GSC is assumed to operate with unitary power factor, ie, $q_r = 0$.

3 | INITIALIZATION METHOD

3.1 | Newton–Raphson approach

The DFIG steady-state model is obtained from Equation 1 (just by neglecting the derivative operator, ie, $p = 0$) and from Equation 2. The resulting set of equations is a nonlinear system, which can be written with the Taylor series (using the first derivative) in the iteration k:

$$\mathbf{F}(\mathbf{x}) = \mathbf{F}(\mathbf{x}_k) + \mathbf{J}(\mathbf{x}_k)\Delta\mathbf{x}, \tag{3}$$

where $\mathbf{F}(\mathbf{x}_k)$ is the linearized system of equations in the iteration k, $\mathbf{J}(\mathbf{x}_k)$ is the Jacobian of the function in the iteration k, ie, the derivative of the function with respect to the variables $\mathbf{x}$, and $\Delta\mathbf{x} = (\mathbf{x}_{k+1} - \mathbf{x}_k)$.

The Newton–Raphson (or NR) algorithm can be used to solve the nonlinear system (Equation 3). It consists of finding the value of the unknown variables $\mathbf{x}$ that meet the following condition:

$$\mathbf{F}(\mathbf{x}) = \mathbf{0}. \tag{4}$$

The procedure to apply the NR algorithm starts by giving initial values to the unknown variables $\mathbf{x}$. Then, the system of Equation 3 is solved. Let $\mathbf{x}_k$ be the value of the unknown variables in the previous iteration, $\mathbf{x}_{k+1}$ the value of the unknown variables in the current iteration, and considering the relation (Equation 4), we can write Equation 3 from the following expression:

$$\mathbf{x}_{k+1} = \mathbf{x}_k - \mathbf{J}^{-1}(\mathbf{x}_k)\mathbf{F}(\mathbf{x}_k). \tag{5}$$

The iterative process is carried out until the iteration in which the error between $\mathbf{x}_{k+1}$ and $\mathbf{x}_k$ is lower than an admissible error ε.

The unknown variables for the DFIG steady-state model are as follows:

$$\mathbf{x} = [i_{sd} \quad i_{sq} \quad i_{rd} \quad i_{rq} \quad v_{rd} \quad v_{rq}]^t. \tag{6}$$

The $\mathbf{F}(\mathbf{x})$ is given by neglecting the derivative term ($p = 0$) of the DFIG equations in Equations 1 and also by active and reactive powers given by Equation 2:

$$\mathbf{F}(\mathbf{x}) = [f_1 \ f_2 \ f_3 \ f_4 \ f_5 \ f_6]^t, \tag{7}$$

which results in the following:

$$
\begin{aligned}
f_1 &= v_{sd} - R_s i_{sd} + L_s \omega_s i_{sq} + M \omega_s i_{rq} \\
f_2 &= v_{sq} - R_s i_{sq} - L_s \omega_s i_{sd} - M \omega_s i_{rd} \\
f_3 &= v_{rd} - R_r i_{rd} + L_r s \omega_s i_{rq} + M s \omega_s i_{sq} \\
f_4 &= v_{rq} - R_r i_{rq} - L_r s \omega_s i_{rd} - M s \omega_s i_{sd} \\
f_5 &= p - v_{sd} i_{sd} - v_{sq} i_{sq} - v_{rd} i_{rd} - v_{rq} i_{rq} \\
f_6 &= q - v_{sq} i_{sd} + v_{sd} i_{sq}
\end{aligned}
\tag{8}
$$

and the Jacobian $\mathbf{J}(\mathbf{x})$ is given by:

$$
\mathbf{J}(\mathbf{x}) = \left[\frac{\partial \mathbf{F}(\mathbf{x})}{\partial i_{sd}} \quad \frac{\partial \mathbf{F}(\mathbf{x})}{\partial i_{sq}} \quad \frac{\partial \mathbf{F}(\mathbf{x})}{\partial i_{rd}} \quad \frac{\partial \mathbf{F}(\mathbf{x})}{\partial i_{rq}} \quad \frac{\partial \mathbf{F}(\mathbf{x})}{\partial v_{rd}} \quad \frac{\partial \mathbf{F}(\mathbf{x})}{\partial v_{rq}} \right] \tag{9}
$$

which results in the following:

$$
\mathbf{J}(\mathbf{x}) = \begin{bmatrix}
-R_s & L_s \omega_s & 0 & M \omega_s & 0 & 0 \\
-L_s \omega_s & -R_s & -M \omega_s & 0 & 0 & 0 \\
0 & M s \omega_s & -R_r & L_r s \omega_s & 1 & 0 \\
-M s \omega_s & 0 & -L_r s \omega_s & -R_r & 0 & 1 \\
-v_{sd} & -v_{sq} & -v_{rd} & -v_{rq} & -i_{rd} & -i_{rq} \\
-v_{sq} & v_{sd} & 0 & 0 & 0 & 0
\end{bmatrix} . \tag{10}
$$

3.2 | Proposed phasor approach

The per-phase steady-state equivalent circuit of a DFIG is depicted in Figure 3A, where $\underline{V}_s$ and $\underline{V}_r$ are the stator and rotor voltage phasors, respectively, $\underline{I}_s$ and $\underline{I}_r$ are the stator and rotor current phasors, respectively, $X_{sl} = X_s - X_m$ is the leakage stator reactance, $X_{rl} = X_r - X_m$ is the leakage rotor **F3**

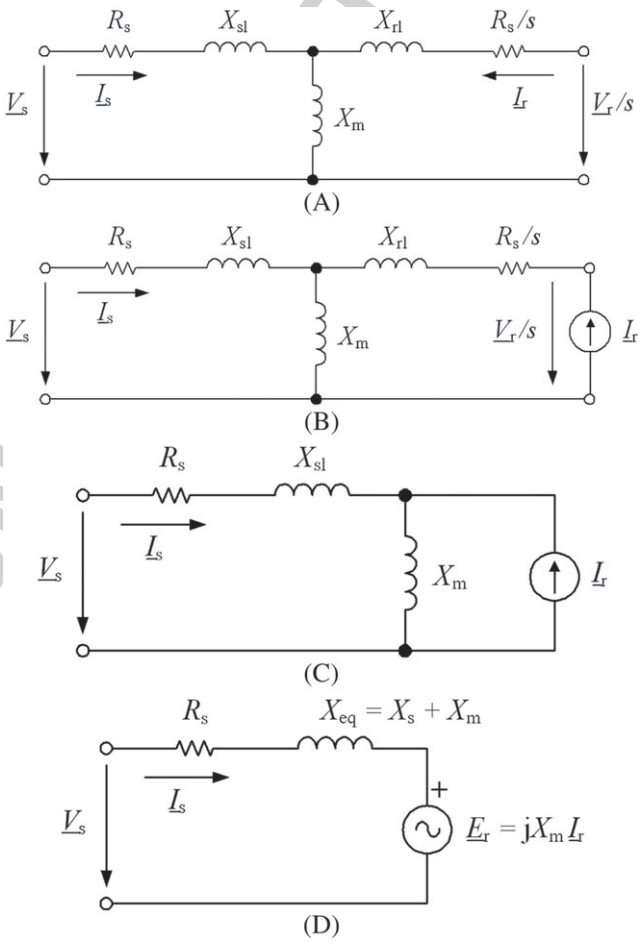

FIGURE 3 Per-phase steady-state equivalent circuit of a doubly fed induction generator. A, General scheme, B, proposed scheme with a current source connected to the rotor, C, simplification, and D, final scheme. Motor sign convention

reactance, R_s and R_r are the stator and rotor resistances, respectively, and s is the DFIG slip. All the represented magnitudes are reduced to the stator, and the motor sign convention has been adopted.

The proposed approach consists on considering a current source connected to the DFIG rotor. This current source models the RSC in Figure 1, assuming that it injects a constant current to the DFIG rotor. The proposed per-phase steady-state equivalent circuit is depicted in Figure 3B. Note that as the current that circulates through the rotor series branch is imposed by the current source, the resulting simplified circuit is depicted in Figure 3C. Finally, the branch that consists of the mutual reactance connected in parallel to the current source can be redrawn by its equivalent voltage source (called $\underline{E}_r$) in series to the mutual reactance, as shown in Figure 3D. The analytical expression for this voltage source is as follows:

$$\underline{E}_r = jX_m\underline{I}_r \ . \tag{11}$$

The equivalent reactance X_{eq} shown in Figure 3D is the series connection between stator reactance and mutual reactance:

$$X_{eq} = X_{sl} + X_m. \tag{12}$$

It should be noted that the proposed per-phase equivalent circuit depicted in Figure 3D reminds us the per-phase equivalent circuit of a synchronous machine. According to the proposed circuit of Figure 3D, the stator current can be obtained by means of the following expression, where R_s is neglected compared with X_{sl} (it is usually an order of magnitude lower[18]):

$$\underline{I}_s = \frac{\underline{V}_s - \underline{E}_r}{jX_{eq}} \ . \tag{13}$$

The apparent power exchanged between the stator of the DFIG and the grid is as follows:

$$\underline{S}_s = 3\underline{V}_s\underline{I}_s^* = 3\underline{V}_s\left(\frac{\underline{V}_s - \underline{E}_r}{jX_{eq}}\right)^* = P_s + jQ_s. \tag{14}$$

Developing the previous equation, we obtain the following expressions for the stator active power (P_s) and for the stator reactive power (Q_s):

$$P_s = -3\frac{V_sE_r\sin\delta}{X_{eq}}, \tag{15}$$

$$Q_s = \frac{3}{X_{eq}}\left(V_s^2 - V_sE_r\cos\delta\right), \tag{16}$$

where the stator voltage is assumed to be the origin of phasors ($\underline{V}_s = V_s0^\circ = V_s$) and the angle of $\underline{E}_r$ is named δ to show its similitude with the load angle in a synchronous machine.

The active power exchanged between the DFIG rotor and the grid corresponds, approximately, with minus s times (s = mechanical slip) the stator power[19]:

$$P_r \approx -sP_s, \tag{17}$$

and the addition of Equations 15 and 17 gives the overall active power exchanged between the DFIG and the grid:

$$P = P_s + P_r = \frac{3(s-1)V_sE_r\sin\delta}{X_{eq}}. \tag{18}$$

The reactive power exchanged between the DFIG rotor and the grid is zero, as the GSC in Figure 1, usually works with unitary power factor. Then, the overall reactive power exchanged between the DFIG and the grid corresponds to the stator reactive power:

$$Q = Q_s + Q_r = \frac{3}{X_{eq}}\left(V_s^2 - V_sE_r\cos\delta\right). \tag{19}$$

The objective of the proposed algorithm is to find the analytical expressions of $\underline{I}_s$, $\underline{I}_r$, and $\underline{V}_r$ in order to initialize the transient regime of the DFIG-based WT, whose dynamic model is given by Equations 1 and 2.

The first step is to obtain the analytical expression for the angle δ. From Equation 18, we obtain the sinus of this angle:

$$\sin\delta = \frac{PX_{eq}}{3(s-1)V_sE_r}, \tag{20}$$

and from Equation 19, we obtain its cosine:

$$\cos\delta = \frac{V_s^2 - QX_{eq}/3}{V_s E_r} \quad . \tag{21}$$

Then, the angle δ is obtained as follows:

$$\delta = \arctan\left(\frac{\sin\delta}{\cos\delta}\right) = \arctan\left(\frac{PX_{eq}}{(s-1)\left(3V_s^2 - QX_{eq}\right)}\right). \tag{22}$$

The second step is to obtain the modulus of $\underline{E}_r$. It can be obtained from Equations 20 and 21 by means of the following trigonometric relationship:

$$\sin^2\delta + \cos^2\delta = 1, \tag{23}$$

which results in the following:

$$E_r = \sqrt{\left(\frac{V_s^2 - QX_{eq}/3}{V_s}\right)^2 + \left(\frac{PX_{eq}}{3(s-1)V_s}\right)^2}. \tag{24}$$

Then, the phasor $\underline{E}_r$ can be written in its rectangular form as follows:

$$\underline{E}_r = \frac{V_s^2 - QX_{eq}/3}{V_s} + j\frac{PX_{eq}}{3(s-1)V_s}. \tag{25}$$

The third step is to obtain the analytical expression for the DFIG rotor current. According to Equations 11 and 25, we can write as follows:

$$\underline{I}_r = -j\frac{\underline{E}_r}{X_m} = \frac{PX_{eq}}{3(s-1)V_s X_m} + j\left(\frac{QX_{eq}/3 - V_s^2}{V_s X_m}\right). \tag{26}$$

The fourth step is to obtain the analytical expression for the DFIG stator current. It can be obtained by applying the Kirchhoff's voltage law to the left mesh of the circuit of Figure 3C (neglecting the stator resistance, as $R_s << X_{sl}$):

$$\underline{V}_s = jX_{sl}\underline{I}_s + jX_m(\underline{I}_s + \underline{I}_r), \tag{27}$$

which results in the following:

$$\underline{I}_s = -\frac{1}{X_{eq}}(X_m\underline{I}_r + j\underline{V}_s), \tag{28}$$

and substituting Equations 26 in 28, it results in the following:

$$\underline{I}_s = -\frac{P}{3(s-1)V_s} - j\frac{Q}{3V_s}. \tag{29}$$

The last step is to obtain the analytical expression for the DFIG rotor voltage, which can be obtained by applying the Kirchhoff's voltage law to the right mesh of the circuit of Figure 3B:

$$\frac{\underline{V}_r}{s} = \underline{I}_r\left(\frac{R_r}{s} + jX_{rl}\right) + jX_m(\underline{I}_s + \underline{I}_r), \tag{30}$$

and substituting Equations 26 and 29 in Equation 30, it results in the following:

$$\begin{aligned}\underline{V}_r = {} & \frac{QX_m s}{3V_s} + \frac{PX_{eq}R_r}{3(s-1)V_s X_m} + \left(\frac{V_s^2 - QX_{eq}/3}{V_s X_m}\right)(X_m + X_{rl})s \\ & + j\left[\left(\frac{sP}{3(s-1)V_s}\right)\left(-X_m + \frac{X_{eq}(X_m + X_{rl})}{X_m}\right) + \frac{R_r}{X_m}\left(\frac{QX_{eq}/3 - V_s^2}{V_s X_m}\right)\right].\end{aligned} \tag{31}$$

Finally, in order to initialize the set of the DFIG dynamic equations given by Equations 1 and 2, the steady-state values of the *dq* components must be calculated. They are easily obtained by means of the previous analytical expressions, as in balanced steady-state conditions, the Park components of a variable *x* can be obtained according to Equation 43 from appendix:

$$x_d = \sqrt{3}X\cos(\varphi_X) = \sqrt{3}\,\mathrm{Re}\{X\}$$
$$x_q = \sqrt{3}X\sin(\varphi_X) = \sqrt{3}\,\mathrm{Im}\{X\}. \tag{32}$$

According to Equation 32, the *dq* components of the DFIG rotor current can be obtained from Equation 26 as follows:

$$i_{rd} = \frac{PX_{eq}}{\sqrt{3}(s-1)V_sX_m} \quad , \quad i_{rq} = \sqrt{3}\frac{QX_{eq}/3 - V_s^2}{V_sX_m}. \tag{33}$$

According to Equation 32, the *dq* components of the DFIG stator current can be obtained from Equation 29 as follows:

$$i_{sd} = \frac{P}{\sqrt{3}(s-1)V_s} \quad , \quad i_{sq} = -\frac{Q}{\sqrt{3}V_s}. \tag{34}$$

Finally, according to Equation 32, the *dq* components of the DFIG rotor voltage can be obtained from Equation 31 as follows:

$$v_{rd} = \sqrt{3}\left[\frac{QX_m s}{3V_s} + \frac{PX_{eq}R_r}{3(s-1)V_sX_m} + \left(\frac{V_s^2 - QX_{eq}/3}{V_sX_m}\right)(X_m + X_{rl})s\right]$$
$$v_{rq} = \sqrt{3}\left[\left(\frac{sP}{3(s-1)V_s}\right)\left(-X_m + \frac{X_{eq}(X_m + X_{rl})}{X_m}\right) + \frac{R_r}{X_m}\left(\frac{QX_{eq}/3 - V_s^2}{V_sX_m}\right)\right]. \tag{35}$$

In summary, the steady-state of the DFIG is defined by the power Equations 18 and 19, the rotor current (Equation 26), the stator current (Equation 29), and the rotor voltage (Equation 31). And the initial conditions for the dynamic analysis of the DFIG are given by the *dq* components of the rotor current (Equation 33), the stator current (Equation 34), and the rotor voltage (Equation 35). It should be noted that the proposed model is only valid for sinusoidal balanced steady-state conditions. If sinusoidal unbalanced conditions take place, then the model should include symmetrical components (both positive-sequence and negative-sequence components) by applying the Fortescue transformation.

4 | CASE STUDY

4.1 | DFIG-based WT parameters

The data of the studied 2-MW WT equipped with DFIG is shown in Table 1 (adapted from Slootweg et al[20]). The maximum power point (MPP) curve from the wind vs the WT speed is given in Figure 4, where A, B, and C are the following operating points: T1 F4

TABLE 1 Characteristics of the wind turbine equipped with doubly fed induction generator (adapted from Slootweg et al[20])

DFIG Rated Values					
U_n (phase-to-phase) = 690 V		f_n = 50 Hz	ω_m = 900–1900 rpm		p = 2
DFIG parameters in pu (U_b = 690 V, S_b = 2 MW and f_b = 50 Hz)					
R_s = 0.01	R_r = 0.01	X_{sl} = 0.1	X_{rl} = 0.08	X_m = 3.0	H_m = 0.5 s
WT parameters					
P_n = 2 MW	$\omega_{t\ n}$ = 18 rpm	$\omega_{t\ min}$ = 9 rpm	$\omega_{t\ max}$ = 19 rpm		H_t = 2.5 s
r = 37.5 m	(radius)	$v_{w\ n}$ = 12 m/s	(rated wind speed)	r_{gb} = 1:100	(gearbox ratio)

Abbreviations: DFIG, doubly fed induction generator; WT, wind turbine.

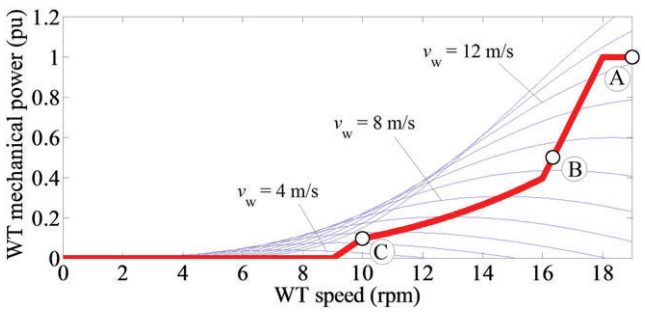

FIGURE 4 Power extracted from the wind (thin blue lines) and optimum power (thick red line) of the wind turbine (WT) equipped with doubly fed induction generator. A, B, and C are the operating points studied in the paper [Colour figure can be viewed at wileyonlinelibrary.com]

- Point A: v_w = 12 m/s, $P = P_n$, and s = −0.27.
- Point B: v_w = 9.3 m/s, P = 0.5 P_n, and s = −0.09.
- Point C: v_w = 5.4 m/s, P = 0.1 P_n, and s = 0.33.

4.2 | DFIG steady-state analysis

The steady-state analysis of the DFIG-based WT will be carried out by means of the two approaches commented in Section 3. Before that, it is necessary to obtain the value of the extracted power from the wind and the value of the DFIG mechanical slip corresponding to this power. For this purpose, the following procedure is followed[14]:

1) Given a known wind speed, v_w, it is possible to obtain the power that can be extracted from this wind speed and its corresponding WT speed from the MPP curve shown in Figure 4. Note that the power extracted from the wind corresponds to the active power delivered by the DFIG, neglecting the power losses in the machine.
2) Knowing the WT speed, ω_t, the mechanical speed of the DFIG, ω_m, can be given by the following equation:

$$\omega_m = \omega_m r_{gb}, \tag{36}$$

where r_{gb} is the gearbox ratio (the mechanical losses in the gearbox have been neglected).

3) Knowing the DFIG speed, ω_m, the mechanical slip, s, is obtained as follows:

$$s = (\omega_s - \wp\omega_m)/\omega_s \tag{37}$$

Once the DFIG slip, s, is known, it is possible to apply either the Newton–Raphson algorithm or the proposed phasor-based expressions in order to solve the DFIG steady-state regime.

Figure 5 shows the procedure to be followed by each approach, and Table 2 shows the obtained results for the three steady-state regimes given by the three WT operating points in Figure 4. The results shown in Table 2 are given in per unit (pu) values, according to the following expressions: F5 T2

$$\begin{aligned} i_{sd\ pu} &= \frac{i_{sd}}{\sqrt{3}I_b}, \quad i_{sq\ pu} = \frac{i_{sq}}{\sqrt{3}I_b}, \quad i_{rd\ pu} = \frac{i_{rd}}{\sqrt{3}I_b}, \\ i_{rq\ pu} &= \frac{i_{rq}}{\sqrt{3}I_b}, \quad v_{rd\ pu} = \frac{v_{rd}}{\sqrt{3}V_b}, \quad v_{rq\ pu} = \frac{v_{rq}}{\sqrt{3}V_b}, \end{aligned} \tag{38}$$

where the base values are U_b = 690 V, S_b = 2 MW and $I_b = S_b/\left(\sqrt{3}U_b\right) = 1673.5$ A.

According to the results shown in Table 2, it is possible to observe that the Newton–Raphson algorithm converges fast (in just 3 iterations the results present an error $\varepsilon < 10^{-4}$). Regarding the proposed approach, it should be observed that in just one iteration (as we only need to apply the phasor equations), we obtain similar results as with the Newton–Raphson approach: just compare the results obtained in the 3rd iteration with the results obtained with the proposed approach. Moreover, it is observed that the required computing time to carry out the simulations is two orders of magnitude smaller in the proposed phasor-based approach than in the traditional Newton–Raphson algorithm.

Then, it can be concluded that the proposed method is easier and faster to implement than the conventional Newton–Raphson algorithm, as it makes use of the phasor expressions and it does not require an iterative process to obtain the final solution, which implies that the computing time required for the simulations is reduced.

4.3 | DFIG dynamic behavior under grid faults

The proposed method to initialize the dynamic study of a DFIG has been simulated considering that the DFIG-based WT starts its operation in steady-state conditions and after a short period of time a three-phase fault is provoked in the power system. This three-phase fault originates a symmetrical voltage sag which is seen in the PCC in Figure 1 as a decrease in the voltage magnitude from its rated value.

A voltage sag is a reduction in the root mean square voltage between 0.1 and 0.9 pu of the prefault voltage between 10 ms (or 0.5 cycles assuming a frequency of 50 Hz) and 1 minute. This definition is stated by the international regulation Institute of Electrical and Electronics Engineers (IEEE) Std 1159–2009 on monitoring electric power quality.[21] Other international standards on voltage sags make reference to achieve immunity on grid connected equipment under voltage sags, such as the International Electrotechnical Commission (IEC) Std 1000-4-11-1004[22] or the regulations set by the CIGRE/CIRED/UIE Working Group on that field.[23] Apart from these international standards, grid operations of Q5 Q6

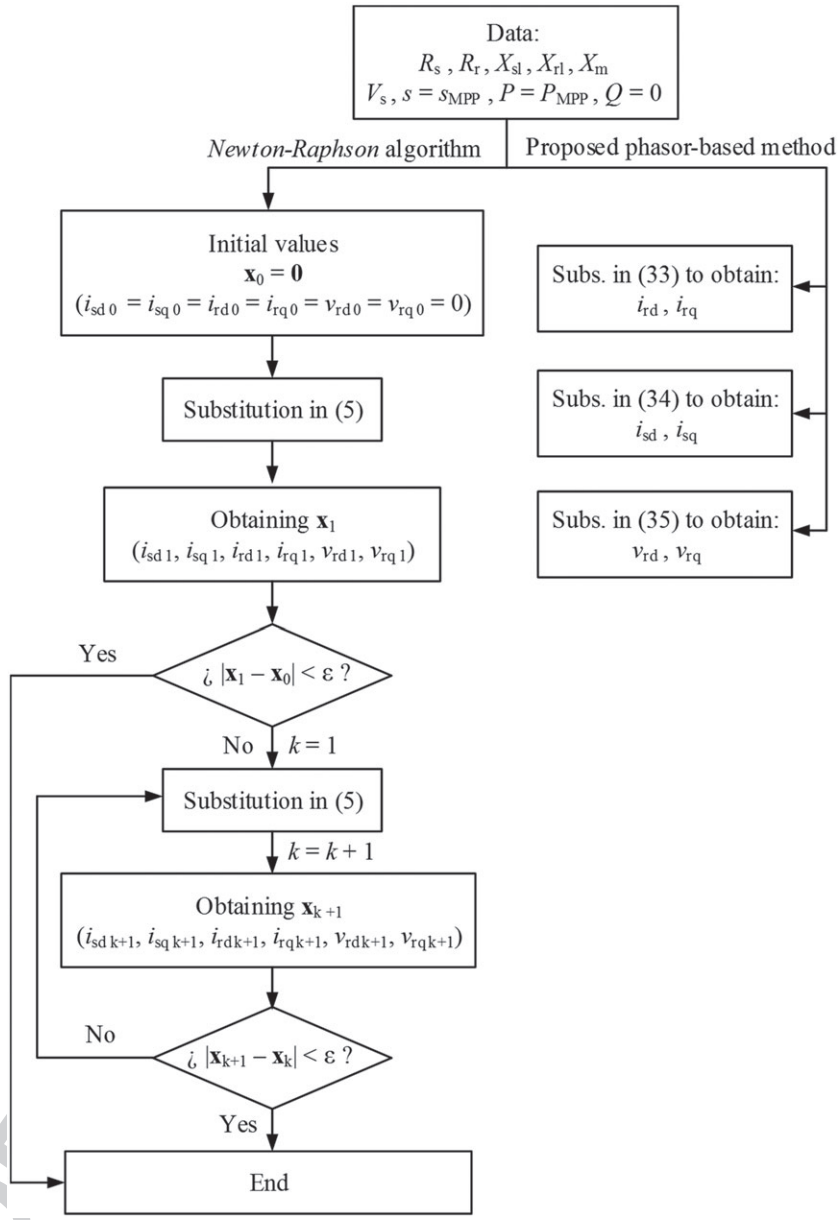

FIGURE 5 Comparison between the Newton-Raphson algorithm (with admissible error ε = 0.0001) and the proposed phasor-based method to solve the steady-state regime of the doubly fed induction generator-based wind turbines, used for the initialization of its dynamic studies

TABLE 2 Doubly fed induction generator steady-state solutions (in pu) under the three wind turbine operating points

WT Operation Point	Iteration Number	Newton–Raphson Algorithm (with Max Adm Error ε = 10^{-4}) [a]						Proposed Phasor-Based Method [b]					
		i_{sd}	i_{sq}	i_{rd}	i_{rq}	v_{rd}	v_{rq}	i_{sd}	i_{sq}	i_{rd}	i_{rq}	v_{rd}	v_{rq}
A	1	−1.000	0	1.033	−0.333	−0.263	−0.052	−0.789	0	0.816	−0.333	−0.266	−0.043
$P = P_n$	2	−0.795	0	0.822	−0.333	−0.266	−0.042	-	-	-	-	-	-
$s = -0.27$	3	−0.796	0	0.822	−0.333	−0.266	−0.042	-	-	-	-	-	-
B	1	−0.500	0	0.517	−0.333	−0.087	−0.011	−0.459	0	0.474	−0.333	−0.087	−0.012
$P = 0.5\ P_n$	2	−0.462	0	0.477	−0.333	−0.087	−0.011	-	-	-	-	-	-
$s = -0.09$	3	−0.462	0	0.477	−0.333	−0.087	−0.011	-	-	-	-	-	-
C	1	−0.096	0	0.099	−0.333	0.343	0.002	− 0.145	0	0.149	−0.333	0.344	0.004
$P = 0.1\ P_n$	2	−0.147	0	0.152	−0.333	0.344	0.006	-	-	-	-	-	-
$s = 0.33$	3	−0.147	0	0.152	−0.333	0.344	0.006	-	-	-	-	-	-

[a] Required computing time (in Matlab™ software): 22.797 ms (for WT operating point A).

[b] Required computing time (in Matlab™ software): 0.134 ms (for WT operating point A).

several countries have developed the so-called grid codes in order to set the conditions in which WTs must remain connected to the grid when voltage sags occur, thus ensuring minimum levels of power quality. Examples of these grid codes are the Danish Eltra & Elkraft's grid code,[24] the German TenneT TSO GmbH's grid code[25] or the Spanish Red Electrica's grid code.[26]

Voltage sags can be characterized by four parameters[27]: depth (h), duration (Δt), phase-angle jump, and fault current angle (ψ). The simulated voltage sag is assumed to have a depth $h = 0.5$, a duration $\Delta t = 5.5$ cycles, and the fault current angle is $\psi = 80°$ (note that this angle varies from 75° to 85° for transmission grids,[28] which is where the DFIG-based WT is connected).

In order to simulate the DFIG-based WT in a simplistic way, the following assumptions have been made:

1) The control can maintain the rotor current constant in the synchronous reference frame; ie, the rotor current during the voltage sag is the same as the steady-state rotor current (the values of this current can be seen in Table 2).
2) The DFIG speed is assumed to be constant, as the voltage sag has a short duration (Δt = 5.5 cycles or 110 ms assuming that the grid frequency is 50 Hz).

According to the aforementioned two assumptions, it is observed that the electrical equations in Equation 1 become a set of differential equations with constant coefficients, where the unknown variable is the transformed stator current (i_{sd} and i_{sq}). As a result, Equation 1 can be solved analytically. This is a good tool to explain and understand the behavior of DFIG-based WTs in order to meet the fault ride-through requirements imposed by grid operators. There are not many analytical studies on DFIGs in the literature. An example of them can be found in López et al,[29,30] where there is no specific control algorithm on the rotor current. In Lima, Luna, Rodríguez, Watanabe, and Blaabjerg, [31] the rotor voltage peak is calculated analytically. Few articles also contemplate the proper design of the proper converter, such as Chondrogiannis Barnes[32] or Hu and He.[33]

The dynamic study of the DFIG-based WT has been carried out considering the three WT operating points in Figure 4, and the represented magnitudes (shown in Figure 6) are follows: *abc* components of the stator current, *abc* components of the rotor current, *abc* components of the rotor voltage, and the electro-magnetic torque. The variables are represented with their per unit (pu) values, considering the following base values: U_b = 690 V, S_b = 2 MW, $I_b = S_b/\left(\sqrt{3}U_b\right) = 1673.5$ A, $\omega_b = 2\pi f_b = 100\pi$ rad/s, and $\Gamma_b = S_b/(\omega_b/\wp) = 12.73$ kNm: F6

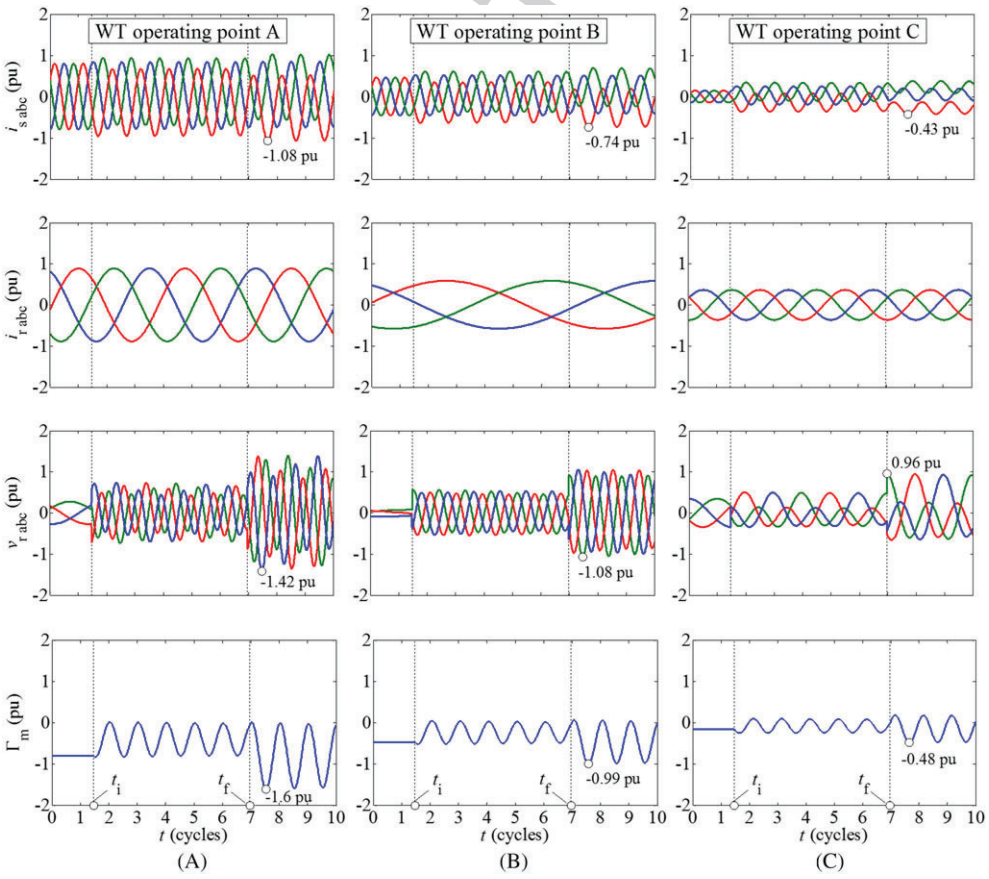

FIGURE 6 Behavior of a wind turbine (WT) equipped with a doubly fed induction generator (assumption of constant rotor current and constant speed) under symmetrical sags caused by three-phase faults. Sag characteristics: h = 0.5, Δt = 5.5 cycles, and ψ = 80°. A, WT operating point A (vw = 12 m/s, P = P_n, and s = −0.27), B, WT operating point B (vw = 9.3 m/s, P = 0.5 P_n, and s = −0.09.), and C, WT operating point C (vw = 5.4 m/s, P = 0.1 P_n, and s = 0.33) [Colour figure can be viewed at wileyonlinelibrary.com]

$$i_{s\,abc\,pu}(t) = \frac{i_{s\,abc}(t)}{\sqrt{2}I_b} \quad , \quad i_{r\,abc\,pu}(t) = \frac{i_{r\,abc}(t)}{\sqrt{2}I_b}$$
$$v_{r\,abc\,pu}(t) = \frac{v_{r\,abc}(t)}{\sqrt{2}V_b} \quad , \quad \Gamma_{m\,pu}(t) = \frac{\Gamma_m}{\Gamma_b} \quad . \tag{39}$$

Figure 6A shows that when the DFIG-based WT operates at its most unfavorable conditions (ie, delivering its rated power to the grid when it rotates at its rated speed), the control strategy lets the stator current peaks be reduced noticeably, as they reach only 8% above the rated value. It is also observed that the rotor current remains constant during the entire transient, as this is the requirement imposed by the proposed control approach. With respect to the rotor voltage, this figure shows that after voltage recovery this variable can exceed values above 40% of the steady-state value. This can be a real problem in ensuring the controllability of the machine, and some limits in the power converter sizing about rotor voltage should be defined. Finally, the electro-magnetic torque shows a 50-Hz oscillation during the voltage sag and a peak of 60% above the steady state value once the fault is cleared. Again, more efforts should be made to reduce these peaks, but this is out of the scope of this paper. With respect to Figure 6b and Figure 6c, the same behavior is revealed, but in these cases, the machine operates delivering 50% and 10% of its rated power, respectively. So the less severe the WT operating point is, the smaller the variable peaks are, which is a logical consequence.

According to the results shown in Figure 6, the following conclusions can be drawn:

1) The proposed method for initialize the dynamic behavior of the DFIG makes it possible to start the simulations at steady-state conditions.
2) The fact of extrapolating the idea of constant rotor current to the entire event (before, during, and after the voltage sag) has resulted in a simple control that makes it possible to reduce the current and torque peaks. This is a really good point, as when voltage sags appear, a proved effect is that there appear both large current and torque peaks,[6,7] which will eventually cause a malfunction of the grid-connected equipment.
3) It can be observed that during the voltage sag, there appear noticeable oscillations in the electro-magnetic torque. These oscillations could be reduced if more sophisticated control algorithm is implemented, which is out of the scope of this paper.

In summary, the presented method based on phasors is a simple approach that can be used to obtain the steady-state values of the Park variables, which are useful to initialize the dynamic studies of a DIFG-based WT. It has also been shown that the fact of considering a constant current in the DFIG rotor is a simple approach to control the DFIG under disturbances, although more studies are needed to validate it. To that purpose, the authors' previous works on DFIG under symmetrical sags,[34] unsymmetrical sags,[35] or under the most severe sags[36] can be consulted, where all sag conditions (durations and depths) have been considered to show the time evolution of the DFIG electro-mechanical variables under a faulty grid. Nevertheless, the advantage of the proposed method is that it helps in the prediction and explanation of the DFIG behavior under voltage sags.

5 | CONCLUSIONS

The present paper has proposed an algorithm to initialize the dynamic studies of WT equipped with DFIG based on solving the steady state by assuming a constant current source in the rotor. This current source models the RSC of the DFIG. The obtained equivalent circuit consists of a voltage source in series with a reactance, which simplifies the analysis of the DFIG. The phasor expressions of the stator current, rotor current, and rotor voltage have been developed, and from these expressions, the steady-state expressions for the *dq* components have been determined.

The proposed method has been compared with the traditional Newton–Raphson algorithm, giving similar results with a negligible error. It has been shown that the proposed method is easier and faster to implement, as it makes use of the phasor expressions and it does not require an iterative process to obtain the final solution that makes it possible a reduction in the computing time to carry out simulations in a software package.

Finally, the obtained steady-state results with the proposed method have been used to initialize the dynamic simulation of a 2-MW WT equipped with DFIG under a faulty grid. Three different WT operating points (given by three different wind speed values) have been considered. In this simulation, the idea of constant rotor current has been kept during the entire event, ie, before, during, and after the fault in order to reduce the current and torque peaks that appear on grid-connected equipment exposed to faults.

The presented study helps in the initialization of DFIG-based WTs for simulation of dynamic studies, making use of a simple and fast approach based on phasors.

ORCID

Alejandro Rolán https://orcid.org/0000-0002-9855-6933

REFERENCES

1. Renewable Energy Policy Network for the 21st Century (REN21). Renewables 2017—global status report. Technical report. March 2017. http://www.ren21.net/gsr-2017/. Accessed June 06, 2018.

2. Mohseni M, Islam S. Review of international grid codes for wind power integration: diversity, technology and a case for global standard. *Renew Sustain Energy Rev*. 2012;16(6):3876-3890.
3. Morren J, De Haan SWH. Ridethrough of wind turbines with doubly-fed induction generator during a voltage dip. *IEEE Trans Energy Convers*. 2005;20(2):435-441.
4. Wasynezuk O, Yi-Min D, Krause PC. Theory and comparison of reduced order models of induction machines. *IEEE Trans Power Syst*. 1985;PAS-104(3):598-606.
5. Ekanayake JB, Holdsworth L, Jenkins N. Comparison of 5th order and 3rd order machine models for doubly fed induction generator (DFIG) wind turbines. *Electr Pow Syst Res*. 2003;67(3):207-215.
6. Guasch L, Córcoles F, Pedra J. Effects of symmetrical and unsymmetrical voltage sags on induction machines. *IEEE Trans Power Delivery*. 2004;19(2):774-782.
7. Pedra J, Sáinz L, Córcoles F, Guasch L. Symmetrical and unsymmetrical voltage sag effects on three-phase transformers. *IEEE Trans Power Delivery*. 2005;20(2):1683-1691.
8. Pena R, Clare JC, Asher GM. Doubly fed induction generator using back-to-back PWM converters and its application to variable-speed wind-energy generation. *IEE Proc–Electr Power Appl*. 1996;143(3):232-241.
9. Kundur P. *Power system stability and control*. New York: McGraw-Hill; 1994.
10. Holdsworth L, Wu XG, Ekanayake JB, Jenkins N. Direct solution method for initialising doubly-fed induction wind turbines in power system dynamic models. *IEE Proc–Gener Transm Distrib*. 2003;150(3):334-342.
11. Vieira JPA, Nunes MVA, Bezerra UH. Analysis of steady-state operation of DFIG-based wind turbines in power systems. In: *Proceedings of the IET Conference on Renewable Power Generation*, Edinburgh, United Kingdom; September 6–8, 2011; 1–5.
12. Medina J, Feijóo A. Calculating steady-state operating conditions for doubly-fed induction generator wind turbines. *IEEE Trans Power Syst*. 2010;25(2):922-928.
13. Feijóo A, Cidrás J, Carrillo C. A third order model for the doubly-fed induction machine. *Electr Pow Syst Res* 2000;56(2):121–127.
14. Slootweg JG, Polinder H, Kling WL. Initialization of wind turbine models in power system dynamics simulations. In: *IEEE Porto Power Tech. Conference*, Porto, Portugal; September 10–13, 2001; 1–6.
15. Amutha N, Kalyan B. Initialization of DFIG based wind generating system. In: *2014 Eighteenth National Power Systems Conference (NPSC)*, Guwahati, India; December 18–20, 2014; 1–5.
16. Wu M, Xie L. Calculating steady-state operating conditions for DFIG-based wind turbines. *IEEE Trans Sustainable Energy*. 2018;9(1):293-301.
17. Han P, Cheng M, Wei X, Jian Y. Steady-state characteristics of the dual-stator brushless doubly fed induction generator. *IEEE Trans Ind Electron*. 2018;65(1):200-210.
18. Lima FKA, Luna A, Rodríguez P, Watanabe EH, Aredes M. Study of a simplified model for DFIG-based wind turbines. In: *Proceedings of the IEEE energy conversion congress and exposition*, ECCE'09, San Jose, USA; September 20–24, 2009; 345–349.
19. Petersson A. *Analysis, Modeling and Control of Doubly-Fed Induction Generators for Wind Turbines*. Ph.D. dissertation. Department of Energy and Environment, Chalmers University of Technology, Göteborg, Sweden, 2005.
20. Slootweg JG, Polinder H, Kling WL. Representing wind turbine electrical generating systems in fundamental frequency simulations. *IEEE Trans Energy Convers*. 2003;18(4):516-524.
21. IEEE Std. 1159-2009: IEEE recommended practice for monitoring electric power quality. IEEE, 2009.
22. IEC Std. 1000-4-11-1994: Test and measurement techniques to verify immunity from voltage dips, interruptions, and variations. IEC, 1994.
23. Bollen, MHJ, Gordon JR, Djokic S, et al. Voltage dip immunity of equipment and installations. CIGRE/CIRED/UIE Working Group C4.110, Tech. Broch. TB-412, Paris, 2010.
24. Eltra & Elkraft. Vindmøller tilsluttet net med spændinger under 100 kV—teknisk forskrift for vindmøllers egenskaber og regulering. May 2004. http://energinet.dk/. Accessed August 28, 2018.
25. TenneT TSO GmbH. Netzanschlussregeln. Hoch- und höchstspannung. December 2012. (English version: Grid code. High and extra high voltage. November 2015). http://www.tennettso.de/. Accessed August 28, 2018.
26. Red Eléctrica de España (REE). *P.O. 12.3* – Requisitos de respuesta frente a huecos de tension de las instalaciones eólicas. October 2006. https://www.boe.es/. Accessed August 28, 2018.
27. Bollen MHJ. *Understanding power quality problems: voltage sags and interruptions*. New York, NY: IEEE Press; 2000.
28. Bollen MHJ. Voltage recovery after unbalanced and balanced voltage dips in three-phase systems. *IEEE Trans Power Delivery*. 2003;18(4):1376-1381.
29. López J, Sanchís P, Roboam X, Marroyo L. Dynamic behavior of the doubly fed induction generator during three-phase voltage dips. *IEEE Trans Energy Convers*. 2007;22(3):709-717.
30. López J, Gubía E, Sanchís P, Roboam X, Marroyo L. Wind turbines based on doubly fed induction generator under asymmetrical voltage dips. *IEEE Trans Energy Convers*. 2008;23(1):321-330.
31. Lima FKA, Luna A, Rodríguez P, Watanabe EH, Blaabjerg F. Rotor voltage dynamics in the doubly fed induction generator during grid faults. *IEEE Trans Power Electron*. 2010;25(1):118-130.
32. Chondrogiannis S, Barnes M. Specification of rotor side voltage source inverter of a doubly-fed induction generator for achieving ride-through capability. *IET Renew Power Gener*. 2008;2(3):139-150.
33. Hu J, He Y. DFIG wind generation systems operating with limited converter rating considered under unbalanced network conditions—analysis and control design. *Renew Energy*. 2011;36(2):829-847.
34. Rolán A, Córcoles F, Pedra J. Doubly fed induction generator subject to symmetrical voltage sags. *IEEE Trans Energy Convers*. 2011;26(4):1219-1229.
35. Rolán A, Córcoles F, Pedra J. Behaviour of the doubly fed induction generator exposed to unsymmetrical voltage sags. *IET Electr Power Appl*. 2012;6(8):561-574.

36. Rolán A, Pedra J, Córcoles F. Detailed study of DFIG-based wind turbines to overcome the most severe grid faults. *Electr Power Energy Syst*. 2014;62:868-878.
37. Park RH. Two-reaction theory of synchronous machines—generalized method of analysis, part I. *AIEE Trans*. 1929;48:716-727.

How to cite this article: Rolán A, Pedra J. Initialization of DFIG wind turbines with a phasor-based approach analysis and comparison with the traditional Newton–Raphson algorithm. *Wind Energy*. 2018;1–13. https://doi.org/10.1002/we.2296

APPENDIX

PARK TRANSFORMATION

The power-invariant (or normalized) form of the Park transformation[37] is defined as follows:

$$\mathbf{P}(\Psi)=\sqrt{\frac{2}{3}}\begin{bmatrix}\frac{1}{\sqrt{2}} & \frac{1}{\sqrt{2}} & \frac{1}{\sqrt{2}}\\ \cos(\Psi) & \cos\left(\Psi-\frac{2\pi}{3}\right) & \cos\left(\Psi+\frac{2\pi}{3}\right)\\ -\sin(\Psi) & -\sin\left(\Psi-\frac{2\pi}{3}\right) & -\sin\left(\Psi+\frac{2\pi}{3}\right)\end{bmatrix}, \tag{40}$$

where Ψ is the transformation angle. By means of this matrix, it is possible to obtain the zero component (0), the direct component (*d*), and the quadrature component (*q*), which are the transformed components of the *abc* components of a variable. If the synchronous reference frame is assumed, the angle that is used to transform the stator variables is $\Psi_s = \omega_s t$, while the angle that is used to transform the rotor variables is $\Psi_r = \Psi_s - \wp\theta_m = s\omega_s t - \wp\theta_{m0}$, where θ_{m0} is the initial mechanical angle (at $t = 0$), which is assumed to be 0. Then, for a given variable $\mathbf{x}$:

$$\begin{aligned}\mathbf{x}_{s\ 0dq} &= \mathbf{P}(\omega_s t)\mathbf{x}_{s\ abc} \quad , \quad \mathbf{x}_{r\ 0dq} = \mathbf{P}(s\omega_s t)\mathbf{x}_{r\ abc}\\ \mathbf{x}_{s\ abc} &= \mathbf{P}(\omega_s t)^{-1}\mathbf{x}_{s\ 0dq} \quad , \quad \mathbf{x}_{r\ abc} = \mathbf{P}(s\omega_s t)^{-1}\mathbf{x}_{r\ 0dq} \quad .\end{aligned} \tag{41}$$

Assuming that the windings (stator and rotor) of the DFIG are isolated Y or Δ connected, the zero components of the transformation are not considered.

Finally, let us assume sinusoidal balanced steady-state conditions. In this case, the *abc* components of any variable *x* are given by:

$$\begin{aligned} x_{sa} &= \sqrt{2}X_s\cos(\omega_s t+\varphi_{x_s}) & x_{ra} &= \sqrt{2}X_r\cos(s\omega_s t+\varphi_{x_r})\\ x_{sb} &= \sqrt{2}X_s\cos\left(\omega_s t+\varphi_{x_s}-\frac{2\pi}{3}\right) & x_{rb} &= \sqrt{2}X_r\cos\left(s\omega_s t+\varphi_{x_r}-\frac{2\pi}{3}\right)\\ x_{sc} &= \sqrt{2}X_s\cos\left(\omega_s t+\varphi_{x_s}-\frac{2\pi}{3}\right) & x_{rc} &= \sqrt{2}X_r\cos\left(s\omega_s t+\varphi_{x_r}+\frac{2\pi}{3}\right)\end{aligned} \tag{42}$$

and substituting Equation 42 in Equation 40, we obtain the *dq* components of the variable under sinusoidal balanced steady-state conditions:

$$\begin{aligned} x_{sd} &= \sqrt{3}X_s\cos(\varphi_{X_s}) \quad , \quad x_{rd} = \sqrt{3}X_r\cos(\varphi_{X_r})\\ x_{sq} &= \sqrt{3}X_s\sin(\varphi_{X_s}) \quad , \quad x_{rq} = \sqrt{3}X_r\sin(\varphi_{X_r})\end{aligned} \tag{43}$$

where the direct (*d*) component of the transformed variable equals the real part of the phasor expression multiplied by $\sqrt{3}$, while the quadrature (*q*) component of the transformed variable equals the imaginary part of the phasor expression multiplied by $\sqrt{3}$.